

Control of a Nonlocal Entanglement in the Micromaser via Two Quanta Non-Linear Processes Induced by Dynamic Stark Shift

M.S. Ateto

Received: 20 April 2008 / Accepted: 6 August 2008 / Published online: 28 August 2008
© Springer Science+Business Media, LLC 2008

Abstract We show that, under certain conditions, the micromaser can act as an effective source of highly correlated atoms. It is possible to create an extended robust entanglement between two successive, initially unentangled atoms passing through a cavity filled with a nonlinear medium taking into consideration a slight level shift. Information is transferred from the cavity to the atoms in order to build up entanglement. The scheme has an advantage over conventional creation of entanglement if the two atoms (qubits) are so far apart that a direct interaction is difficult to achieve. The interaction of the atoms with the micromaser occurs under the influence of a two-quantum transition process. Interesting phenomena are observed, and an extended robust entangled state is obtained for different values of the system parameters. Illustrative variational calculations are performed to demonstrate the effect within an analytically tractable two-qubit model.

Keywords Micromaser · Nonlocal entanglement · Two-qubits · Two-quantum process · Concurrence · Nonlinear media · Stark shift

1 Introduction

Entanglement usually arises from quantum correlations between separated subsystems that cannot be created by local actions on each subsystem. Preparation of quantum entanglement between distant parties is an important task required for quantum communication and quantum information processing [1]. In such processing one usually needs to find the entanglement properties and a way to control it, therefore the study of the dynamic properties of entanglement is useful for processing quantum information.

M.S. Ateto (✉)
Mathematics Department, Faculty of Science, South Valley University, 83523 Qena, Egypt
e-mail: omersog@yahoo.com

Present address:

M.S. Ateto
Theoretisch-Physikalisches Institut, Friedrich-Schiller-Universität Jena, Max-Wien-Platz 1, 07743 Jena, Germany

In the last years there has been an intensive research in the field of quantum communication that has yielded a variety of methods to distribute bipartite entanglement [2–15]. Nevertheless, due to the lack of a complete understanding of mixed state entanglement and multi-partite entanglement, it is not always clear what is the optimal way to distribute entanglement among distant parties.

A great effort has been devoted to the generation of atomic entanglement and entanglement between cavity modes through atom-photon interactions [16–36] and some notable experimental demonstrations have also been performed, for instance Refs. [37–49]. Of particular interest is the generation of entangled states in two-atom systems, since they can represent two qubits, the building blocks of the quantum gates that are essential to implement quantum protocols in quantum information processing.

A number of studies have shown that entanglement can be created between two objects that do not interact directly with each other, but interact with a common field, heat bath or thermal cavity field [26, 48–50]. The formation of atom-photon entanglement and the subsequent generation of correlations between spatially separated atoms have been shown using the micromaser [41, 43–47, 51–56].

The micromaser [57–59] is appreciated as a practical device for processing information. It stores radiation for times significantly longer than the duration of the interaction with any single atom [57]. The interaction of an atom with the intracavity field of a micromaser will leave the atom-field system in an entangled state. The long cavity lifetime implies that the memory of this entanglement can influence the interaction with subsequent atoms and nonlocal correlations between these successive atoms can be induced leading to a violation of Bells inequality [57]. In other words, the successive atoms can interact with the field left by earlier atoms, in this manner gain can be seen with the most diffuse of gain media containing, on average, less than one atom at any given moment [60] and the dynamics of an atom inside the cavity will modify the evolution of the later atoms [53–56, 61].

For a field that is interacting with more than one atom at a time, the atom-field entanglement was investigated [36]. In this scheme [36], an atom of fixed position situated at a peak of the cavity field becomes entangled with a second atom, at a variable distance away from the first atom, via their mutual cavity field with which they interact. Furthermore, the entanglement between a pair of atoms pumped at the same time through a micromaser has been analyzed in Ref. [41]. In practice it is rather difficult to realize such a setup though. The genuine one-atom micromaser, on the other hand, can be operated over a reasonably large region of parameter space, and is thus a feasible device [53–56] for generating entanglement between two or more atoms.

It has become well known that the degree of quantum entanglement depends crucially on the physical nature of the interacting objects and the character of their mutual coupling. It has been noticed that the above investigations involved mostly the absorption or emission of a single photon in an atomic transition. However, involvement of more than one photon, in particular, two photons in the transition between two atomic levels has been known for a long time [62–64]. The output radiation from such interactions exhibits nonclassical properties such as strong sub-Poissonian photon statistics as well as fields with increased photon number [65]. Needless to say, the idea of squeezed light has originated from two-photon process [66, 67]. Thus, it would be interesting to study the properties of two-atom entanglement in the framework of a two-photon process. Moreover, the two-photon process introduces a dynamic Stark shift in the atomic transition which is related to the magnitude of the electric field of the radiation inside the cavity.

However, it should be noticed that all these results have been obtained for the case where the Kerr medium and the Stark shift are ignored. The Kerr medium [68–71] can be modelled

as an anharmonic oscillator with frequency ω . Physically this model may be realized as if the cavity contains two different species of atoms, one of which behaves like a two-level atom and the other behaves like an anharmonic oscillator in the single-mode field of frequency ω [72]. Such a model is interesting by itself. The cavity mode is coupled to the Kerr medium as well as to the two-level atoms.

A Kerr-like medium can be useful in many respects, such as detection of nonclassical states [73], quantum nondemolition measurement [74], investigation of quantum fluctuations [75], generation of entangled macroscopic quantum states [76, 77], and quantum information processing [78, 79].

In a previous study [50] it has been shown that the entanglement between two qubits that do not interact directly with each other can be created for a very short time after the interaction is switched on.

Our purpose here is to demonstrate analytically the increase of the entanglement time created for two atoms (qubits) if the cavity field is filled with a nonlinear medium and a slight level shift is taken into consideration. In Sect. 2, we introduce our model and the obtained wave function that controls the model in a general form at time $t > 0$. A brief discussion of the technique we are going to use to compute the entanglement (concurrence) of mixed quantum states is introduced in Sect. 3. The reduced density matrices of some special cases of our final state vector at any time $t > 0$ depending on various initial states of the system are computed in Sect. 4, supported by discussions of the study. Our conclusions are summarized in Sect. 5.

2 The Full System and Its Solution

We consider a scheme of the micromaser-type where two two-level atoms traverse a high- Q ($Q \approx 10^9$) single-mode cavity one after the other in a manner that their flights through the cavity do not overlap [26, 39, 51, 52, 57, 80–83]. There is no direct interaction between the two atoms, although secondary correlations develop between them. The entanglement of their wave functions with the cavity photons can be used to formulate local-realist bounds on the detection probabilities for the two atoms [51, 57]. The generation of nonlocal correlations between the two atomic states emerging from the cavity can in general be understood using the Horodecki theorem [84]. The cavity mode is assumed to be filled with a Kerr-like medium [68–71]. Each atom has energy levels $|1_i\rangle$ and $|0_i\rangle$ ($i = 1, 2$) such that $E_{1_i} - E_{0_i} = \hbar\omega_0$. We assume that the two atoms make individually two-photon transitions of frequency 2ω between the nondegenerate states $|0_i\rangle$ (the ground state, energy E_{0_i} , $i = 1, 2$) and $|1_i\rangle$ (the excited state, energy E_{1_i}). The transitions are mediated by a single intermediate level $|k\rangle$ (energy E_k , with $E_{1_i} > E_k > E_{0_i}$); the frequencies for $|0_i\rangle \rightarrow |k\rangle$ and $|1_i\rangle \rightarrow |k\rangle$ are $\omega - \Delta$ and $\omega + \Delta$, respectively. The frequency ω_0 includes a spontaneous contribution to Stark shift due to a direct dipole transition from the intermediate level $|k\rangle$ to $|0_i\rangle$ and $|1_i\rangle$. The coupling constants κ_1 (for $|0_i\rangle \rightarrow |k\rangle$), κ_2 (for $|1_i\rangle \rightarrow |k\rangle$), and Δ determine the Stark shift parameters β_1 and β_2 of the two levels and also the coupling κ between the effective two level atoms, states $|0_i\rangle$ and $|1_i\rangle$, and the field mode

$$\beta_1 = \kappa_1^2 \Delta^{-1}, \quad \beta_2 = \kappa_2^2 \Delta^{-1}, \quad \kappa = \kappa_1 \kappa_2 \Delta^{-1}. \quad (1)$$

The atom-field interaction is governed by the Jaynes-Cummings (JC) model via a two-quantum process [68, 69, 85]. It is assumed that the atom-field interaction time is shorter than the lifetime of the cavity, so that the cavity relaxation will not be considered. The cavity field is assumed to be filled with a nonlinear medium, namely, Kerr medium [68–71],

while the atoms are assumed to have a shift in their levels due to the interaction with the radiation field. Assuming for simplicity the photon mode to be in resonance with the atoms, the model Hamiltonian under the rotating wave approximation (RWA) reads

$$\hat{H} = \omega_0 \hat{S}_3 + \omega \hat{A}^\dagger \hat{A} + \chi \hat{A}^{\dagger 2} \hat{A}^2 + \frac{1}{2} \hat{A}^\dagger \hat{A} [\beta_1 (1 - \hat{S}_3) + \beta_2 (1 + \hat{S}_3)] + \kappa (\hat{A}^{\dagger 2} \hat{S}_- + \hat{A}^2 \hat{S}_+) \quad (\hbar = 1), \tag{2}$$

where ω is the cavity frequency, $\omega_0 = 2\omega$ is the frequency of two atomic energy level difference and $\kappa = \kappa_1 \kappa_2 \Delta^{-1}$ is the coupling parameter that connects the field with the atomic system. We denote by χ the dispersive part of the third-order susceptibility of the Kerr-like medium [68–71]. The operator \hat{A}^\dagger (\hat{A}) is the field creation (annihilation) operator, which satisfies the commutation relation $[\hat{A}, \hat{A}^\dagger] = 1$. The operators \hat{S}_+ , \hat{S}_- and \hat{S}_3 are the usual raising, lowering and inversion operators for the two-level atomic system, which satisfy the commutation relations $[\hat{S}_3, \hat{S}_\pm] = \pm 2\hat{S}_\pm$ and $[\hat{S}_+, \hat{S}_-] = \hat{S}_3$. The Hamiltonian given by (2) can be written in the form

$$\hat{H} = \hat{H}_0 + \hat{H}_{int}, \tag{3}$$

where H_0 represents the unperturbed Hamiltonian that is given by

$$\hat{H}_0 = \omega (\hat{A}^\dagger \hat{A} + \hat{S}_3), \tag{4}$$

while the perturbed Hamiltonian is given by

$$\hat{H} = \chi \hat{A}^{\dagger 2} \hat{A}^2 + \frac{1}{2} \hat{A}^\dagger \hat{A} [\beta_1 (1 - \hat{S}_3) + \beta_2 (1 + \hat{S}_3)] + \kappa (\hat{A}^{\dagger 2} \hat{S}_- + \hat{A}^2 \hat{S}_+). \tag{5}$$

The state vector $|\psi_f(t = 0)\rangle$ of the field is represented by a linear superposition of the number state $|n\rangle$, i.e.,

$$|\psi_f(t = 0)\rangle = \sum_{n=0}^{\infty} F_n |n\rangle, \tag{6}$$

where $|n\rangle$ is an eigenstate of the number operator $\hat{A}^\dagger \hat{A} = n$; $\hat{A}^\dagger \hat{A} |n\rangle = n |n\rangle$, and F_n is, in general, complex and gives the probability of the field to have n photons by the relation

$$P(n) = \langle n | \psi_f(t = 0) \rangle \langle \psi_f(t = 0) | n \rangle = |F_n|^2. \tag{7}$$

As already indicated above, we consider a pair of two-level atoms going through the cavity mode one after another. Then the initial state vector of the interacting first atom-field system is given by

$$|\psi_{a-f}(t = 0)\rangle = |\psi_a(t = 0)\rangle \otimes |\psi_f(t = 0)\rangle = \sum_{n=0}^{\infty} F_n |n, 1_1\rangle, \tag{8}$$

where $|1_1\rangle$ represents the state vector of the first atom being in excited state. At any instant of time t the joint state vector of the field and the first atom can be obtained from the solution of the time-dependent Schrödinger equation

$$i \frac{d}{dt} |\psi_{a-f}(t)\rangle = \hat{H} |\psi_{a-f}(t)\rangle. \tag{9}$$

The time of flight through the cavity t is the same for every atom [26, 39, 51, 52, 57, 80–83], and the joint state vector of both the two atoms and the field may be denoted by $|\psi_{a-a-f}(t)\rangle$, and the corresponding atom-atom-field pure-state density operator is

$$\rho(t) = |\psi(t)\rangle\langle\psi(t)|; \quad |\psi(t)\rangle = |\psi_{a-a-f}(t)\rangle. \tag{10}$$

In order to quantify the degree of entanglement between the two atoms, the field variables must be traced out. One may write the reduced mixed-state density matrix of the two atoms after taking the trace over the field variables as

$$\rho_{a-a}(t) = \text{Tr}_{\text{field}} \rho(t). \tag{11}$$

Under the initial condition (6), by solving the Schrödinger equation (9), we obtain directly the time-dependent wave function of the atom-field system that evolves according to the form

$$|\psi_{a-f}(t)\rangle = \sum_n^\infty F_n e^{-it\Lambda_n} [K_n(t) |n, 1_1\rangle + R_{n+2}(t) |n + 2, 0_1\rangle], \tag{12}$$

with the amplitudes $K_n(t)$ and $R_n(t)$ given by

$$K_n(t) = \cos(\Upsilon_n t) + i\kappa \left[\frac{\chi}{\kappa} (2n + 1) + \frac{n(r^2 - 1) + 2r^2}{2r} \right] \frac{\sin(\Upsilon_n t)}{\Upsilon_n}, \tag{13}$$

and,

$$R_{n-2}(t) = -i\kappa \sqrt{n(n-1)} \frac{\sin(\Upsilon_{n-2} t)}{\Upsilon_{n-2}}, \tag{14}$$

where Υ_n is given by

$$\Upsilon_n = \kappa \sqrt{\left[\frac{\chi}{\kappa} (2n + 1) + \frac{n(r^2 - 1) + 2r^2}{2r} \right]^2 + (n + 1)(n + 2)}, \tag{15}$$

and Λ_n reads

$$\Lambda_n = \kappa \left[\frac{\chi}{\kappa} n(n + 1) + \frac{n(r^2 + 1) + 2r^2}{2r} \right], \tag{16}$$

with $r = \kappa_1/\kappa_2$.

Note that within the delay time between the two atoms the field evolves towards a thermal steady state, moreover, repetition of the instant in which the later atoms enter the cavity means the same field repeats at this instants precisely when successive atoms exit the cavity [58].

If an additional atom is prepared in a superposition as

$$|\psi_a(t > 0)\rangle_0 = a|1_2\rangle + (a - 1)^2|0_2\rangle, \tag{17}$$

this atom will interact with the field that has been modified by the passage of the first atom. Assuming the flight time t of the two atoms through the cavity to be the same, the joint time-evolved wave vector of the tripartite system of the two atoms and the cavity system after the second atom leaves the cavity is obtained by solving the Schrödinger equation

$$i \frac{d}{dt} |\psi_{a-a-f}(t)\rangle = H_{int} |\psi_{a-a-f}(t)\rangle, \tag{18}$$

which is expressed as

$$\begin{aligned}
 |\psi_{a-a-f}(t)\rangle = & \sum_n F_n \{ a (e^{-2it\Lambda_n} [H_n(t)|n, 1_1, 1_2\rangle + T_{n+2}(t)|n + 2, 1_1, 0_2\rangle] \\
 & + e^{-it\Lambda_{n+2}} e^{-it\Lambda_n} [J_{n+2}(t)|n + 2, 0_1, 1_2\rangle + V_{n+4}(t)|n + 4, 0_1, 0_2\rangle]) \\
 & \times (a - 1)^2 (e^{-it\Lambda_n} e^{-it\Lambda_{n-2}} [W_n(t)|n, 1_1, 0_2\rangle + X_{n-2}(t)|n - 2, 1_1, 1_2\rangle]) \\
 & + e^{-2it\Lambda_n} [Y_{n+2}(t)|n + 2, 0_1, 0_2\rangle + Z_n(t)|n, 0_1, 1_2\rangle] \}, \tag{19}
 \end{aligned}$$

where the amplitudes $H_n(t)$, $T_{n+1}(t)$, $J_{n+1}(t)$, $V_{n+2}(t)$, $W_n(t)$, $X_{n-2}(t)$, $Y_{n+2}(t)$, and $Z_n(t)$ are given by

$$H_n(t) = [K_n(t)]^2, \tag{20}$$

$$T_{n+2}(t) = K_n(t)R_{n+2}(t), \tag{21}$$

$$J_{n+2}(t) = K_{n+2}(t)R_{n+2}(t), \tag{22}$$

$$V_{n+4}(t) = R_{n+2}(t)R_{n+4}(t). \tag{23}$$

$$W(n, t) = K_n(t)K_{n-2}^*(t), \tag{24}$$

$$X_{n-2}(t) = K_n(t)R_n(t), \tag{25}$$

$$Y_{n+2}(t) = K_n^*(t)R_{n+2}(t), \tag{26}$$

and

$$Z_n(t) = [R_{n+2}(t)]^2, \tag{27}$$

respectively.

3 Entanglement Measure

For bipartite pure states, the partial (von Neumann) entropy of the reduced density matrices can provide a good measure of entanglement. However, for mixed states von Neumann entropy fails, because it can not distinguish classical and quantum mechanical correlations. For mixed states, the entanglement can be measured as the average entanglement of its pure-state decompositions $E_f(\rho)$

$$E_f(\rho) = \min \sum_i p_i E(\psi_i), \tag{28}$$

with $E(\psi_i)$ being the entanglement measure for the pure state ψ_i corresponding to all the possible decompositions $\rho = \sum_i p_i |\psi_i\rangle\langle\psi_i|$. The existence of an infinite number of decompositions makes their minimization over this set difficult. Wootters [24] succeeded in deriving an analytical solution to this difficult minimization procedure in terms of the eigenvalues of the non-Hermitian operator

$$R = \rho \tilde{\rho}, \tag{29}$$

where the tilde denotes the spin-flip of the quantum state, which is defined as

$$\tilde{\rho} = (\sigma_y \otimes \sigma_y)\rho^*(\sigma_y \otimes \sigma_y), \tag{30}$$

where σ_y is the Pauli matrix, and ρ^* is the complex conjugate of ρ where both are expressed in a fixed basis such as $\{|e\rangle, |g\rangle\}$.

In terms of the eigenvalues of $R = \rho\tilde{\rho}$, $E_f(\rho)$ (known as the entanglement of formation) takes the form

$$E_f(\rho) = H\left[\frac{1}{2} + \frac{1}{2}\sqrt{1 - C^2(\rho)}\right], \tag{31}$$

where $C(\rho)$ is called the concurrence and is defined as:

$$C(\rho) = \max\left(0, \sqrt{\lambda_1} - \sqrt{\lambda_2} - \sqrt{\lambda_3} - \sqrt{\lambda_4}\right), \tag{32}$$

with the λ 's representing the eigenvalues of $R = \rho\tilde{\rho}$ in descending order and

$$H(z) = -z \log z - (1 - z) \log(1 - z) \tag{33}$$

is the binary entropy. The concurrence is associated with the entanglement of formation $E_f(\rho)$, (31), but it is by itself a good measure for entanglement. The range of concurrence is from 0 to 1. For unentangled atoms $C(\rho) = 0$ whereas $C(\rho) = 1$ for maximally entangled atoms.

We consider special cases of the initial conditions, namely (i) only one atom excited; and (ii) initially both atoms excited.

We apply two different excitations of the initial field, namely Fock state excitation and thermal field excitation.

4 Special Cases

4.1 Case 1. Excitation in a Fock State

If the field is excited in a Fock state, the amplitudes F_n in (6) obey the relation

$$F_n = \delta_{m,n}, \tag{34}$$

where m is the photon number of Fock state.

4.1.1 Only One Excited Atom

By setting $a = 0$ in (17) and $F_n = \delta_{m,n}$ in (19), we obtain the wave function of the system with field excited in a Fock state and with initially excited atom followed by an atom in the ground state.

Having obtained the wave function of the full system, the corresponding density operator of the total system can be easily obtained using (10). The atom-atom system can be described in the basis of product states of the individual atoms

$$|1_1, 0_2\rangle = |1\rangle, \tag{35a}$$

$$|1_1, 1_2\rangle = |2\rangle, \quad (35b)$$

$$|0_1, 0_2\rangle = |3\rangle, \quad (35c)$$

$$|0_1, 1_2\rangle = |4\rangle. \quad (35d)$$

Applying (11) to obtain the reduced density operator of the two atoms, which can be written in this basis as

$$\begin{aligned} \rho_{a-a}(t) = & \rho_{11}(t)|1\rangle\langle 1| + \rho_{14}(t)|1\rangle\langle 4| + \rho_{22}(t)|2\rangle\langle 2| \\ & + \rho_{33}(t)|3\rangle\langle 3| + \rho_{41}(t)|4\rangle\langle 1| + \rho_{44}(t)|4\rangle\langle 4|, \end{aligned} \quad (36)$$

with

$$\rho_{11}(t) = |W_n(t)|^2, \quad (37)$$

$$\rho_{14}(t) = e^{-i\kappa\left[2\frac{\kappa}{\kappa}(2n-1) + \frac{\kappa^2+1}{2r}\right]t} W_n(t) Z_n^*(t) = \rho_{41}^*(t), \quad (38)$$

$$\rho_{22}(t) = |X_{n-2}(t)|^2, \quad (39)$$

$$\rho_{33}(t) = |Y_{n+2}(t)|^2, \quad (40)$$

$$\rho_{44}(t) = |Z_n(t)|^2. \quad (41)$$

Expressing the reduced density state (36) in matrix form as

$$\rho_{a-a}(\mathbf{t}) = \begin{pmatrix} \rho_{11} & 0 & 0 & \rho_{14} \\ 0 & \rho_{22} & 0 & 0 \\ 0 & 0 & \rho_{33} & 0 \\ \rho_{41} & 0 & 0 & \rho_{44} \end{pmatrix}, \quad (42)$$

one may write the spin-flip reduced density state $\tilde{\rho}$ of ρ by applying (30) in the form

$$\tilde{\rho}_{a-a}(\mathbf{t}) = \begin{pmatrix} \rho_{44} & 0 & 0 & \rho_{41} \\ 0 & \rho_{33} & 0 & 0 \\ 0 & 0 & \rho_{22} & 0 \\ \rho_{14} & 0 & 0 & \rho_{11} \end{pmatrix}. \quad (43)$$

From an easy procedure one can obtain the square roots of the eigenvalues of the matrix R , given by (29), which are expressed by the set

$$\begin{aligned} \{\sqrt{\lambda_i}\} = & \left\{ \sqrt{\rho_{22}\rho_{33}}, \sqrt{\rho_{22}\rho_{33}}, \operatorname{Re}(\rho_{14}) + \sqrt{\rho_{11}\rho_{44} - [\operatorname{Im}(\rho_{14})]^2}, \right. \\ & \left. \operatorname{Re}(\rho_{14}) - \sqrt{\rho_{11}\rho_{44} - [\operatorname{Im}(\rho_{14})]^2} \right\}. \end{aligned} \quad (44)$$

As found above, one may use the largest eigenvalue using (32) to obtain the concurrence $C(\rho)$ as

$$C(\rho) = 2\left(\sqrt{\rho_{11}\rho_{44} - [\operatorname{Im}(\rho_{14})]^2} - \sqrt{\rho_{22}\rho_{33}}\right). \quad (45)$$

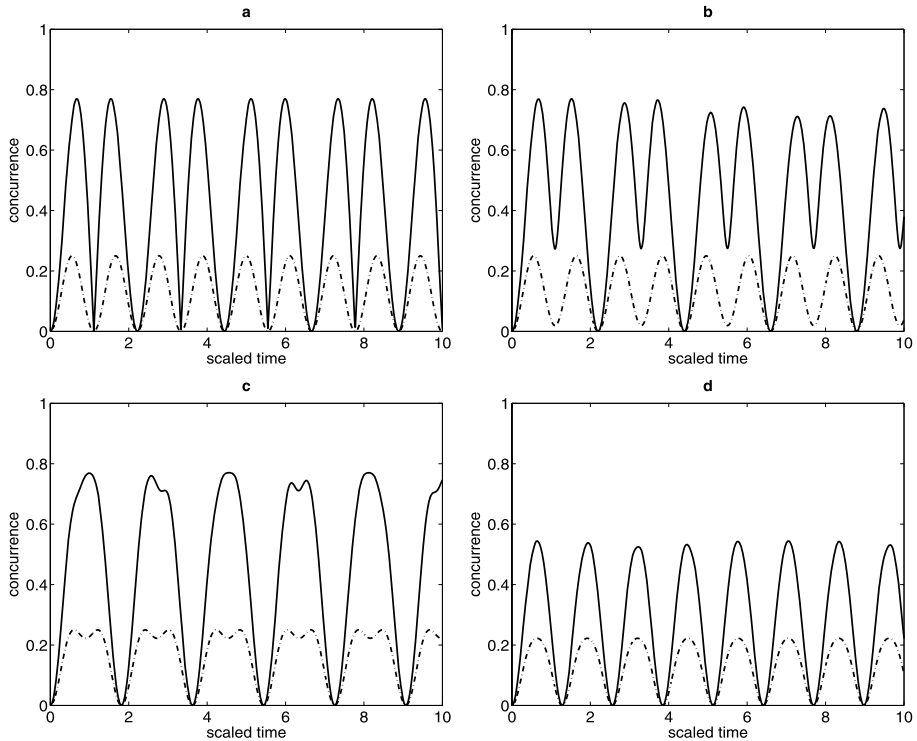


Fig. 1 Concurrence C (solid curve) and $\rho_{22} + \rho_{33}$ (dotted curve) as functions of the scaled time κt . The cavity field start from a Fock state with $n = 0.0$ where $r = 0.0$. **(a)** $\chi/\kappa = 0.0$. **(b)** $\chi/\kappa = 0.2$. **(c)** $\chi/\kappa = 1.0$. **(d)** $\chi/\kappa = 2.0$

One of the interesting phenomenon described by two-level system is the dynamical behavior. In the following, we examine the creation of entanglement in a system that consisting of a pair of two-level atoms mediated by quantum field contained in a cavity through which the two atoms pass successively. For the case when the initially excited atom is followed by the atom in the ground state, the resulting entanglement, measured by the concurrence C , as well as the sum of the populations $\rho_{22} + \rho_{33}$ are depicted in Figs. 1, 2, 3 and 4. We examine the effects of the level shifts as well as of the Kerr-like medium on the creation of entanglement between the two atoms mediated by the cavity field initially prepared in a Fock state. The case of the effective vacuum is quite interesting since in this case C oscillates between zeros and its maximum value (see Fig. 1a). It shows a two-peak periodical behavior with maxima ≈ 0.8 that are reached at the maxima of $\rho_{22} + \rho_{33}$ which also shows periodical behavior with maxima ≈ 0.25 . In this case, the concurrence C reduces to $C = 2\sqrt{\rho_{11}\rho_{44}}$ where $\rho_{22} = 0$ and ρ_{14} is always real. In fact, C attains the value zero (corresponding to disentangled atoms) when $\rho_{22} + \rho_{33} = 0$ (corresponding to atoms in pure state) while strong entanglement occurs at $\rho_{22} + \rho_{33} = 0.25$ (corresponding to atoms in coherent atomic state). It is worth mentioning that a similar behavior was shown in Ref. [80], for one-quantum process, but with more oscillations in the same interval of time. As soon as we apply the nonlinear medium, an interesting result can be observed. The splitting disentanglement point of the two peaks begins to disappear gradually by increasing χ/κ till χ/κ reaches unity, which shows one

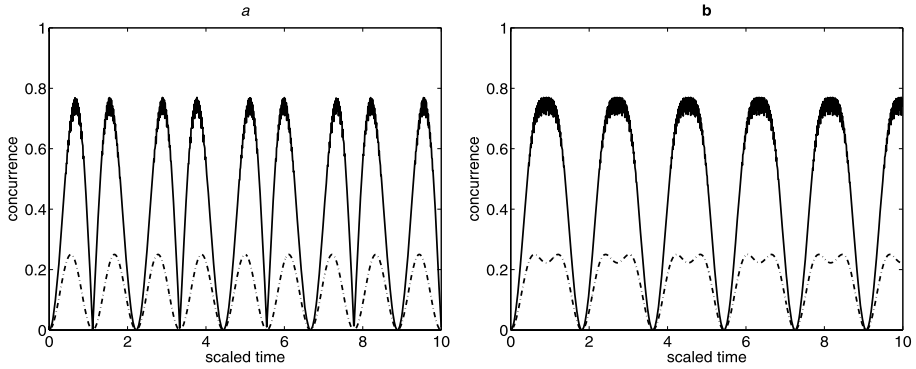


Fig. 2 The same as Fig. 1 but for (a) $\chi/\kappa = 0.0, r = 0.001$. (b) $\chi/\kappa = 1.0, r = 0.001$

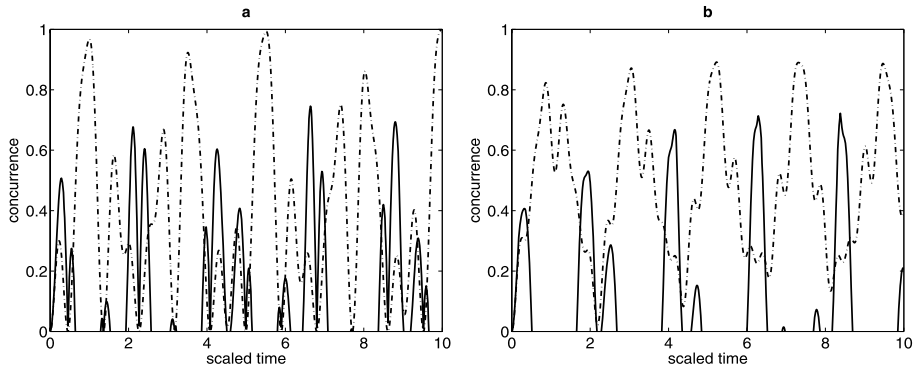


Fig. 3 The same as Fig. 1 but when $n = 2.0$, (a) $\chi/\kappa = 0.0$. (b) $\chi/\kappa = 0.5$

peak periodical behavior in approximately same time intervals, Figs. 1b and 1c. Moreover, the same behavior is also observed for $\rho_{22} + \rho_{33}$. In this case, the atomic system exhibits long time intervals of entanglement with strong Kerr medium. This is because the fact that the higher values of the Kerr parameter allow a complete transmission of the interaction field incident on the atomic system. A very strong Kerr medium decreases the entanglement maxima, while the periodical behavior is preserved (see Fig. 1d). The above results show that the two atoms exhibit long time intervals of entanglement the application of Kerr medium with matching Kerr parameter.

An interesting case is the one when we assume that $\kappa_2 \gg \kappa_1$ so that the coupling parameter ratio, $r = \frac{\kappa_1}{\kappa_2} < 10^{-2}$, where the effect of one of the coupling parameters is very weak (see Fig. 2a).

We notice that C as well as $\rho_{22} + \rho_{33}$ evolve identically with fixed-amplitude periodical evolution. Moreover, C shows two-peak oscillatory behavior with maxima ($\simeq 0.8$) that are reached at the maxima of $\rho_{22} + \rho_{33}$, Fig. 2a. Also, C shows very small rapid oscillations around its maxima before it collapses to its minimum (see Fig. 2a). This implies a longer time of strong entanglement between the two atoms. When the Stark shift parameter r increases, a considerable decrease of the maxima of C is found comparing with that of $\rho_{22} + \rho_{33}$, especially when $r = 0.2$, similar to the effect of very high Kerr parameter, Fig. 1d.

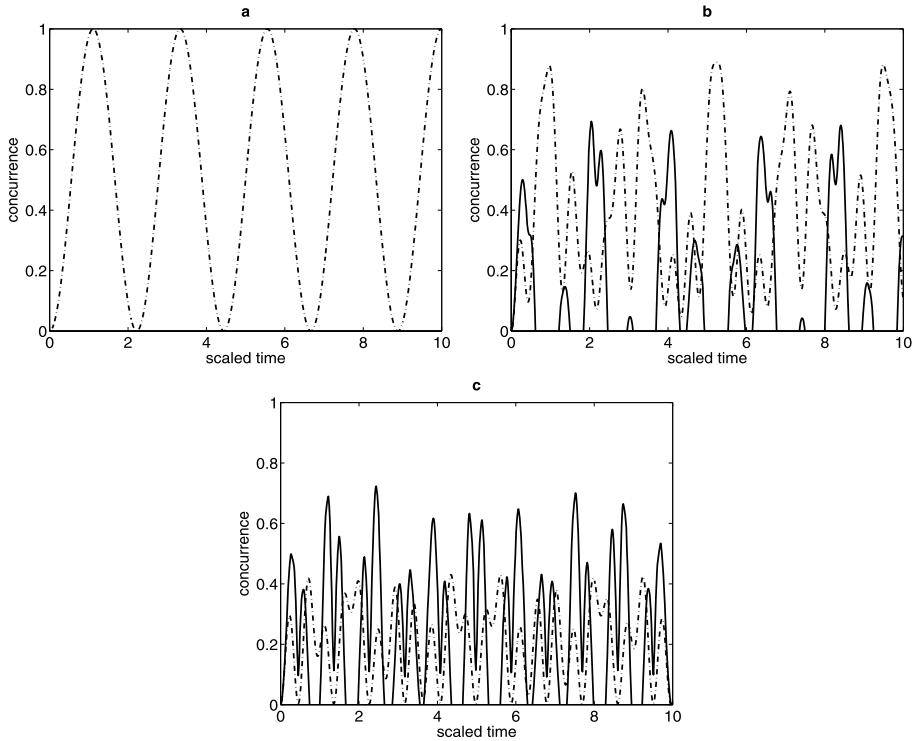


Fig. 4 Concurrence C (solid curve) and $\rho_{22} + \rho_{33}$ (dotted curve) as functions of the scaled time κt . The cavity field start from a Fock state with $n = 2.0$ where $\chi/\kappa = 0.0$. (a) $r = 0.001$. (b) $r = 0.5$. (c) $\chi = 2.0$, $r = 0.1$

Further interesting results are found when we take into account the effects of both Kerr and Stark parameters. One peak periodical behavior with clearly remarkable interval (\approx twice the case when no Kerr and stark) of time with very small rapid oscillations around C maxima (Figs. 1a, 2b). In this case the two atoms are in the entangled state for longer periods of time than in the previous cases before collapse to disentangled state. When $n = 2.0$, C falls off rapidly except for some revivals in irregular intervals with the minima of C being reached at the maxima of $\rho_{22} + \rho_{33}$ (Fig. 3a). Moreover, a weak stark constant, $r = 0.5$, reduces the revival intervals with a remarkable reduction of the C maxima, Fig. 3b.

A surprising result is found when the excitation number $n = 2.0$, while $\frac{\kappa_1}{\kappa_2} < 10^{-2}$. The two atoms remain in a pure state forever although the populations sum oscillates periodically with time with maxima equal to unity. In this case, due to the strong tendency of the ground atom to become excited, its interaction with the field dominates, while neither interaction between field and the excited atom (since no role of its level shifts) nor the two atoms themselves. In this case, the atomic states oscillates between $|1_1, 0_2\rangle$ and $|1_1, 1_2\rangle$, i.e., both probabilities ρ_{11} and ρ_{22} contribute to C , while ρ_{33} , ρ_{44} and $\text{Im}[\rho_{14}]$ are always zero, which implies $C = 0$ in all times (Fig. 4a). So we do not need a full population to get strong entanglement between the two atoms as illustrated in Fig. 1a which shows the opposite behaviors of $\rho_{22} + \rho_{33}$ and C , i.e., the smaller the populations sum, the higher the concurrence and stronger entanglement between the atoms. With increasing r , a kind of entanglement between the two atoms is created due to the role of the level shifts of both atoms. It is evi-

dent that the strongest degree of entanglement occurs when $\rho_{22} + \rho_{33}$ reaches its minimum. Moreover, the amplitudes of both C and $\rho_{22} + \rho_{33}$ decrease considerably as $|r| > 1$. A case with high Kerr parameter, $\chi/\kappa = 2.0$, with values of $r = 0.1$ is considered in Fig. 4c, which shows the tendency of both atoms to be entangled more quickly with the maxima ($\simeq 0.75$) being reached when $\rho_{22} + \rho_{33} = 0.25$ and any value of $\rho_{22} + \rho_{33}$ less or greater than this value means low degree of entanglement between the two atoms.

4.1.2 Two Excited Atoms

By setting $F_n = \delta_{m,n}$ and $a = 1$, we obtain the wave function of the system with field excited initially in a Fock state and with initially the two atoms are excited. In this case, the atom-atom system can be described in the basis

$$|1_1, 1_2\rangle = |1\rangle, \quad (46a)$$

$$|1_1, 0_2\rangle = |2\rangle, \quad (46b)$$

$$|0_1, 1_2\rangle = |3\rangle, \quad (46c)$$

$$|0_1, 0_2\rangle = |4\rangle, \quad (46d)$$

where the reduced density operator of the two atoms can be written in this basis as

$$\begin{aligned} \rho_{a-a}(t) = & \rho_{11}(t)|1\rangle\langle 1| + \rho_{22}(t)|2\rangle\langle 2| + \rho_{33}(t)|3\rangle\langle 3| \\ & + \rho_{23}(t)|2\rangle\langle 3| + \rho_{32}(t)|3\rangle\langle 2| + \rho_{44}(t)|4\rangle\langle 4|, \end{aligned} \quad (47)$$

$$\rho_{11}(t) = |H_n(t)|^2, \quad (48)$$

$$\rho_{22}(t) = |T_{n+2}(t)|^2, \quad (49)$$

$$\rho_{23}(t) = e^{i\kappa[2\frac{\chi}{\kappa}(2n+3) + \frac{r^2+1}{r}]t} T_{n+2}(t) J_{n+2}^*(t) = \rho_{32}^*(t), \quad (50)$$

$$\rho_{33}(t) = |J_{n+2}(t)|^2, \quad (51)$$

$$\rho_{44}(t) = |V_{n+4}(t)|^2. \quad (52)$$

One may write $\rho_{a-a}(t)$ in the form

$$\rho_{a-a}(\mathbf{t}) = \begin{pmatrix} \rho_{11} & 0 & 0 & 0 \\ 0 & \rho_{22} & \rho_{23} & 0 \\ 0 & \rho_{32} & \rho_{33} & 0 \\ 0 & 0 & 0 & \rho_{44} \end{pmatrix}, \quad (53)$$

while the spin-flip reduced density operator $\tilde{\rho}$ can be obtained by applying (30)

$$\tilde{\rho}_{a-a}(\mathbf{t}) = \begin{pmatrix} \rho_{44} & 0 & 0 & 0 \\ 0 & \rho_{33} & \rho_{32} & 0 \\ 0 & \rho_{23} & \rho_{22} & 0 \\ 0 & 0 & 0 & \rho_{11} \end{pmatrix}, \quad (54)$$

and the square roots of the eigenvalues of the matrix R , given by (29), are the following

$$\{\sqrt{\lambda_i}\} = \left\{ \text{Re}(\rho_{23}) + \sqrt{\rho_{22}\rho_{33} - [\text{Im}(\rho_{23})]^2}, \text{Re}(\rho_{23}) - \sqrt{\rho_{22}\rho_{33} - [\text{Im}(\rho_{23})]^2}, \sqrt{\rho_{11}\rho_{44}}, \sqrt{\rho_{11}\rho_{44}} \right\}. \tag{55}$$

By using of (32) to obtain the largest eigenvalue, the concurrence $C(\rho)$ takes the from

$$C(\rho) = \max\left(0, \sqrt{\lambda_1} - \sqrt{\lambda_2} - \sqrt{\lambda_3} - \sqrt{\lambda_4}\right) = 2\left(\sqrt{\rho_{22}\rho_{33} - [\text{Im}(\rho_{23})]^2} - \sqrt{\rho_{11}\rho_{44}}\right). \tag{56}$$

To obtain a clear understanding of the situation we examine the concurrence and population dynamics when both successive atoms enter the cavity initially in an excited state. In vacuum, one can clearly notice the strong positive effect of the nonlinear medium on the degree of entanglement of the atomic system. When the Kerr parameter is absolutely zero, the maximum degree of entanglement ($\simeq 0.75$) is reached near the end of the scaled time (at $t \simeq 8/\kappa$) where the two atoms in some kind of opposite states. Moreover, by increasing the value of the Kerr parameter, $\chi/\kappa = 0.5$, the concurrence begins with maximum $C \simeq 0.72$ is reached in the near the begin of time scale with wider intervals of entanglement of the atomic system (Figs. 5a, b).

On taking into consideration the Stark shift, the obtained results are illustrated in Fig. 6. We can notice clearly the similar behavior as in Sect. 4.1.1 except for that C reaches its minimum where $\rho_{22} + \rho_{33} = 1.0$, and when $r = 0.2$, little small shift parameter, a quasi-periodical behavior with wider temporal intervals of atomic entanglement are showed due to the Stark shift in opposite to its effect in corresponding case. When the cavity is excited with number state $n = 2$, and $\chi/\kappa = 0.0$, $\chi/\kappa = 0.5$, we notice the strong positive effect of the excitation number on the entanglement of the atomic system. We can clearly notice more oscillations of C in the same time intervals, see Fig. 7. This implies that the Kerr medium acts as factor of enhancement of the entanglement between the two atoms in opposite to the

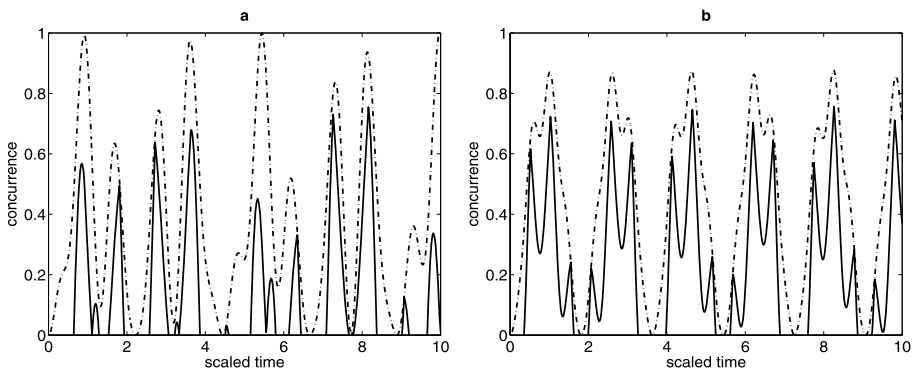


Fig. 5 Concurrence C (solid curve) and $\rho_{22} + \rho_{33}$ (dotted curve) as functions of the scaled time κt . The cavity field start from a Fock state with $n = 0.0$ where $r = 0.0$. (a) $\chi/\kappa = 0.0$. (b) $\chi/\kappa = 1.0$

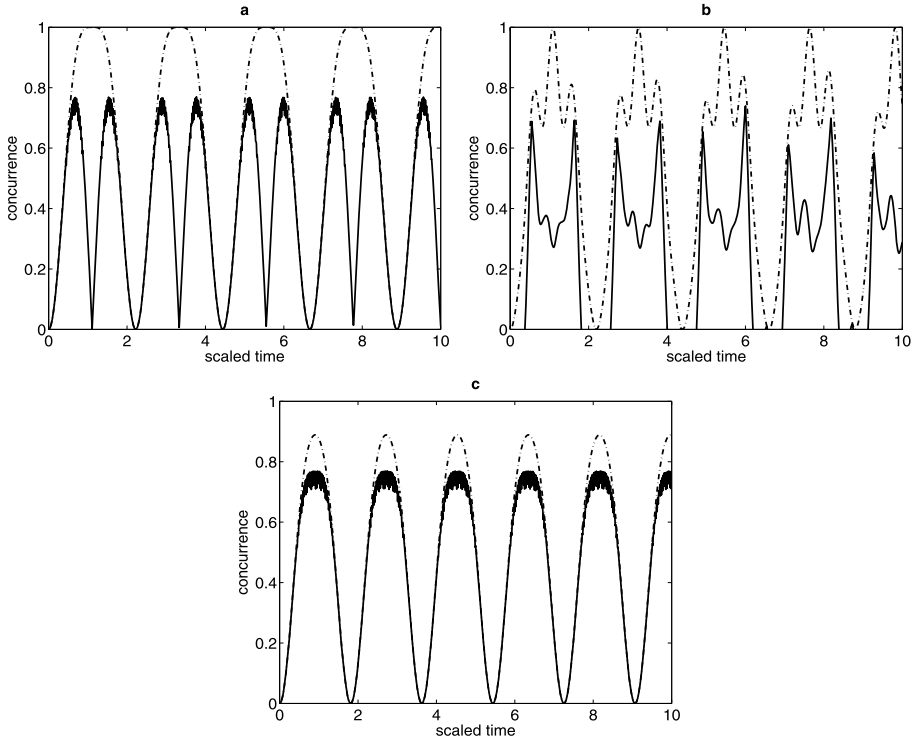


Fig. 6 The same as Fig. 5, but for $\chi/\kappa = 0.0$. (a) $r = 0.001$. (b) $r = 0.2$. (c) $\chi/\kappa = 1.0$, $r = 0.001$

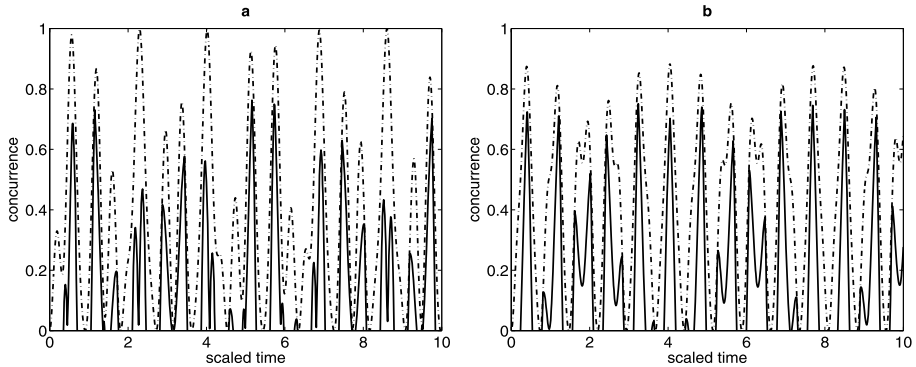


Fig. 7 The same as Fig. 5, but for $n = 2.0$ and $\chi/\kappa = 0.5$ for (b)

same situation of one cavity Fock state [80]. Moreover, the maxima of C depend crucially on the maxima of $\rho_{22} + \rho_{33}$.

More surprising is the case when $\frac{\kappa_1}{\kappa_2} < 10^{-2}$, in this case, $\rho_{11} \simeq 1.0$, while $\rho_{22}, \rho_{33}, \rho_{44}$ and $\text{Im}[\rho_{23}]$ are always zero, which implies that the two atoms remain in their initial excited states and the cavity field plays no role and entanglement of the two atoms is not observed. As the atomic system has a level shift, the atomic system shows entanglement whose max-

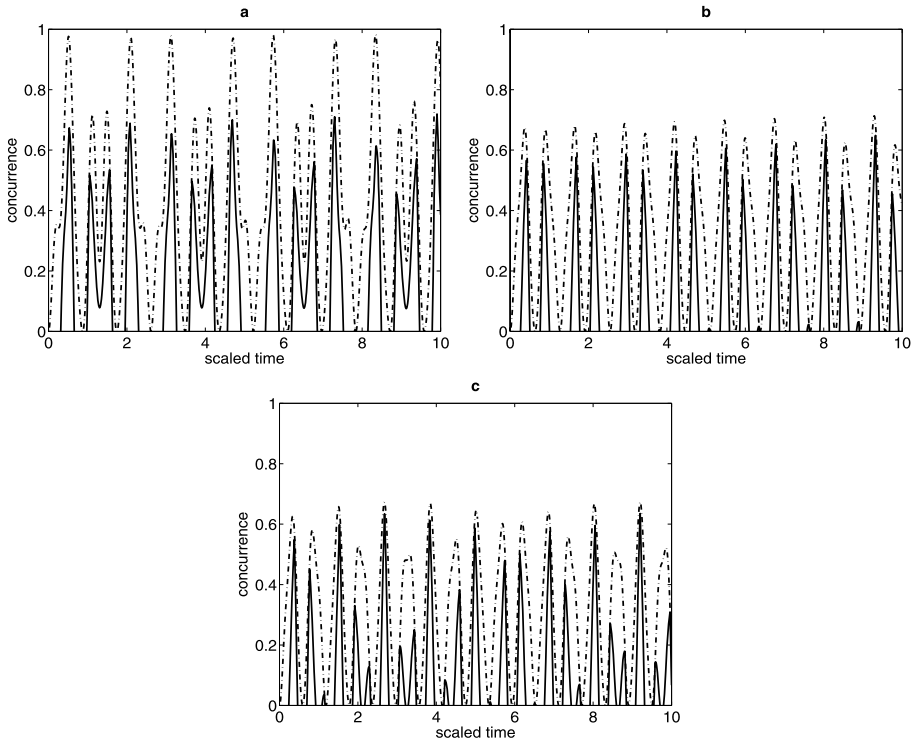


Fig. 8 Concurrence C (solid curve) and $\rho_{22} + \rho_{33}$ (dotted curve) as functions of the scaled time κt . The cavity field start from a Fock state with $n = 2.0$ where $\chi/\kappa = 0.0$. **(a)** $r = 0.5$. **(b)** $r = 2.0$. **(c)** $\chi/\kappa = 0.1$, $r = 2.0$

ima are reached at the maxima of $\rho_{22} + \rho_{33}$. The entanglement amplitude decreases as the Stark shift parameter increases and as possible as the Kerr parameter is still small, see Fig. 8.

Opposite to the case of only one excited atom, when $n > 0$, the number of photons in the cavity destroys the entanglement between the two atoms in case of small Stark shift. As the level shift between the two atomic levels increases, more intervals of entanglement between the atoms are created associated with increasing of the maxima of C which occur at the maxima of $\rho_{22} + \rho_{33}$ till $r = 2.0$ by which a periodical evolution of C appears.

4.2 Case 2. Excitation in a Thermal State

The thermal field is the most easily available radiation field. At thermal equilibrium, the field has an average photon number given by

$$\bar{n} = (e^{\hbar\omega/kT} - 1)^{-1}, \tag{57}$$

with Boltzmann constant k and absolute temperature T . The photon distribution $p(n)$ is given by

$$p(n) = \frac{\bar{n}^n}{(1 + \bar{n})^{n+1}}, \tag{58}$$

which has a peak at zero, i.e., $n_{peak} = 0$.

4.2.1 Only One Excited Atom

Setting $F_n = F_n \delta_{n,n}$ and $a = 0$ the wave function that governs the system in a thermal state, with initially excited atom followed by the one in the ground state, can be obtained. With the condition that $p(n) = |F_n|^2$ is the photon distribution function of the thermal cavity given by (58), the reduced density operator of the atom-field system after taking the trace over the field variables has the form of (36) with the coefficients given by

$$\rho_{11}(t) = \sum_n p(n) |W_n(t)|^2, \tag{59}$$

$$\rho_{14}(t) = \sum_n p(n) e^{-i\kappa [2\frac{\chi}{\kappa}(2n-1) + \frac{r^2+1}{2r}]t} W_n(t) Z_n^*(t) = \rho_{41}^*(t), \tag{60}$$

$$\rho_{22}(t) = \sum_n p(n) |X_{n-2}(t)|^2, \tag{61}$$

$$\rho_{33}(t) = \sum_n p(n) |Y_{n+2}(t)|^2, \tag{62}$$

$$\rho_{44}(t) = \sum_n p(n) |Z_n(t)|^2. \tag{63}$$

With these elements, following the same procedure, one can easily compute the concurrence $C(\rho)$ given by (32).

In the following we compare the results obtained when the cavity field is excited in the thermal field with various mean photon numbers. The results are depicted in Figs. 9, 10, 11 and 12.

A small average photon number, $\bar{n} = 0.5$ creates a high degree of entanglement of chaotic behavior of the atomic system with many maxima of the highest value ($\simeq 0.88$) is reached when $\rho_{22} + \rho_{33} = 0.0$. Moreover, the atomic system remains entangled forever, Fig. 9a.

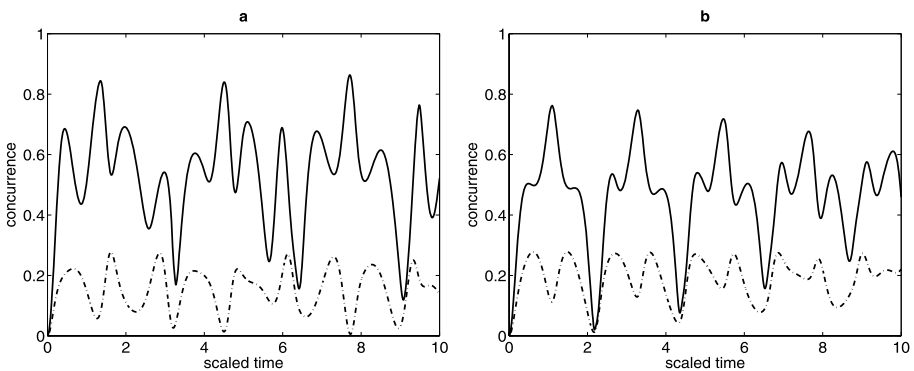


Fig. 9 Concurrence C (solid curve) and $\rho_{22} + \rho_{33}$ (dotted curve) as functions of the scaled time κt . The cavity field start from a thermal state with average photon number $\bar{n} = 0.5$ where $r = 0.0$. (a) $\chi/\kappa = 0.0$. (b) $\chi/\kappa = 0.5$

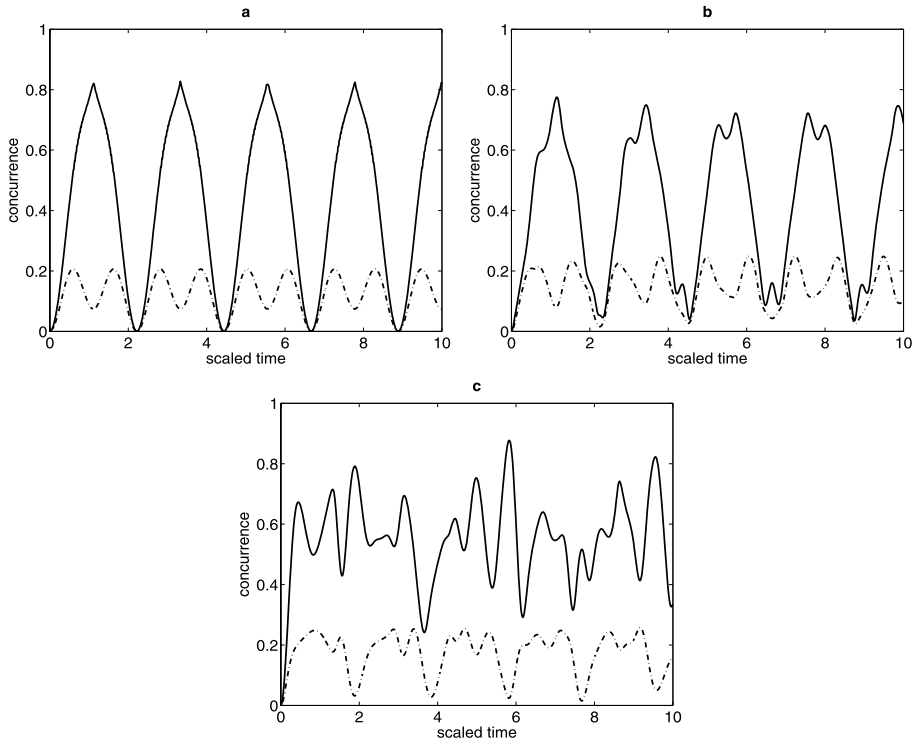


Fig. 10 The same as Fig. 9 but for $\chi/\kappa = 0.0$. (a) $r = 0.01$. (b) $r = 0.1$. (c) $\chi/\kappa = 0.5, r = 0.3$

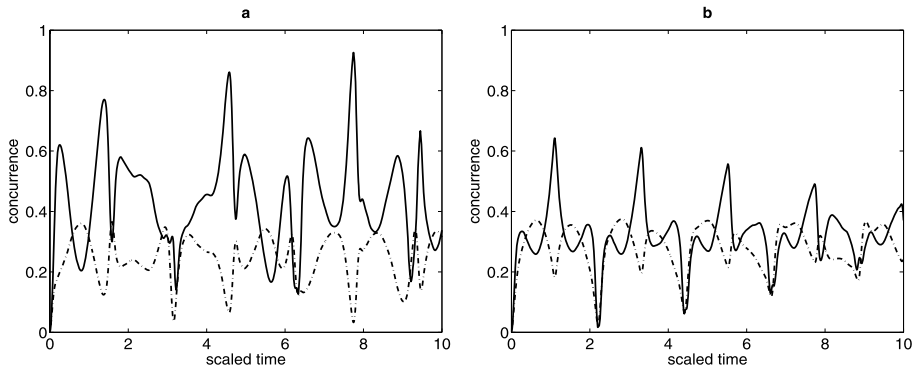


Fig. 11 The same as Fig. 9 but for $\bar{n} = 2.0$

A similar effect can be noticed by increasing the average photon number, $\bar{n} = 2.0$, with higher degree of entanglement $C \simeq 0.93$ accompanied by increase of its minima, Fig. 11a. Choosing a Kerr parameter of value $\chi/\kappa = 0.5$, affects the general behavior of C negatively, where C goes to zero after one period of $\rho_{22} + \rho_{33}$, while its maxima are remarkably reduced.

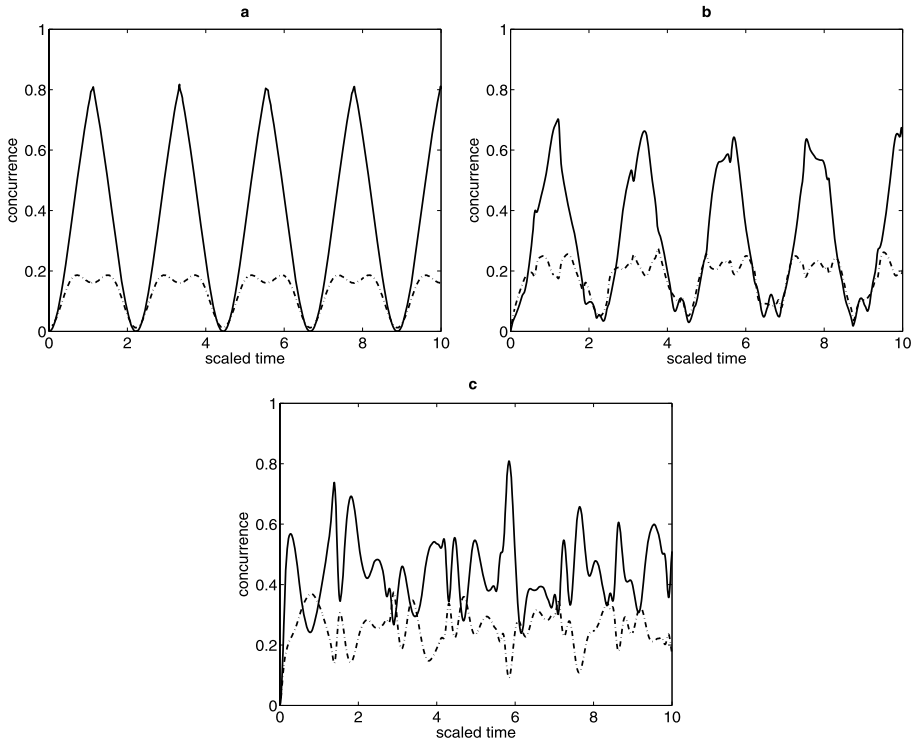


Fig. 12 The same as Fig. 10 but for $\bar{n} = 2.0$

However, increasing \bar{n} decreases the maxima of C remarkably while the general behavior is preserved, see Fig. 11b.

A Stark shift with parameter $r < 10^{-2}$ creates periodical entanglement with maxima ($\simeq 0.82$) with period $t = 0.7n\pi/\kappa$, $n = 0, 1, 2, \dots$ collapse to minima slower than when $\bar{n} = 2.0$, see Figs. 10a, 12a.

Increasing the shift parameter, $r = 0.1$, reduces the maxima of C , while a quasi-periodical behavior can be noticed while similarly to the case of $\bar{n} = 2.0$, the state of the two atoms is not a pure stste, except for the case when the maxima of C reduce remarkably, Figs. 10b, 12b.

When the effects of both Kerr-like medium and Stark shift are taken into account, the only noticeable effect is the reduction of the minima of C while the general behavior as the case when no stark is present, Fig. 9c, 12d.

4.2.2 Two Excited Atoms

To obtain the wave function of this case, we set $F_n = F_n\delta_{n,n}$ and $a = 1$ in (19). With the same condition $p(n) = |F_n|^2$, the reduced density state of the atom-system after taking the trace over the field variables has the form of (28) with the coefficients given by

$$\rho_{11}(t) = \sum_n p(n)|H_n(t)|^2, \tag{64}$$

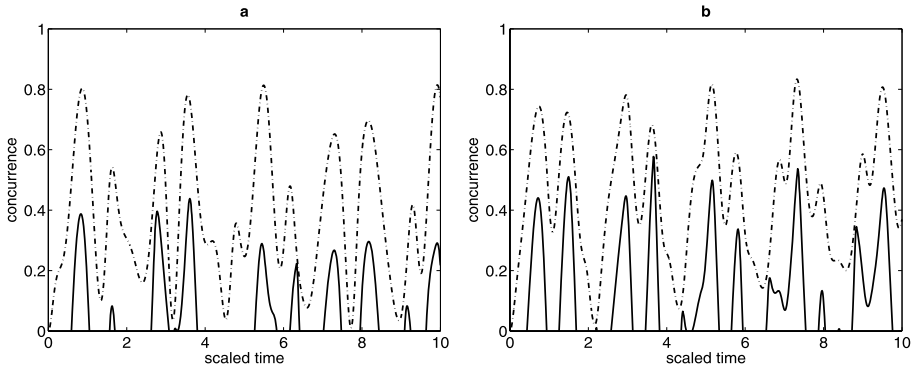


Fig. 13 Concurrence C (solid curve) and $\rho_{22} + \rho_{33}$ (dotted curve) as functions of the scaled time κt . The cavity field start from a thermal state with average photon number $\bar{n} = 0.5$ where $r = 0.0$. **(a)** $\chi/\kappa = 0.0$. **(b)** $\chi/\kappa = 0.5$

$$\rho_{22}(t) = \sum_n p(n) |T_{n+2}(t)|^2, \tag{65}$$

$$\rho_{23}(t) = \sum_n p(n) e^{i\kappa[2\frac{\chi}{\kappa}(2n+3) + \frac{t^2+1}{r}t]} T_{n+2}(t) J_{n+2}^*(t) = \rho_{32}^*(t), \tag{66}$$

$$\rho_{33}(t) = \sum_n p(n) |J_{n+2}(t)|^2, \tag{67}$$

$$\rho_{44}(t) = \sum_n p(n) |V_{n+4}(t)|^2. \tag{68}$$

With these elements the concurrence $C(\rho)$ can be easily computed.

Remarkably interesting results are found when the injected thermal field interacts with two atoms passing through it in excited states. The results are shown in Figs. 13, 14, 15, and 16. We notice clearly the average photon number reducing the general behavior of the concurrence C , while similar behaviors to the corresponding cases of Fock state field are noticed. Moreover, the effect of nonlinear medium on increasing the maxima of C , and creating a periodical entanglement with small oscillations around its maximum with wider periods by taking into account the effect of level shifts are preserved. Also, the behavior of C , where reaches its maxima at the maxima of $\rho_{22} + \rho_{33}$ is also preserved, see Figs. 13–16 and 5–8.

5 Conclusion

In conclusion, from the results illustrated in the previous sections, we can conclude that two atoms (two-qubits) entanglement via two-photon process is more sensitive to the initial conditions than one photon process. Long-time intervals of two-qubit entanglement can be achieved by filling the vacuum cavity with a Kerr-like medium with parameter close to unity and taking into account a slight level shift regardless of the initial states of the two atoms. Moreover, when the cavity contains only one atom excited, long-time periods of two-qubits

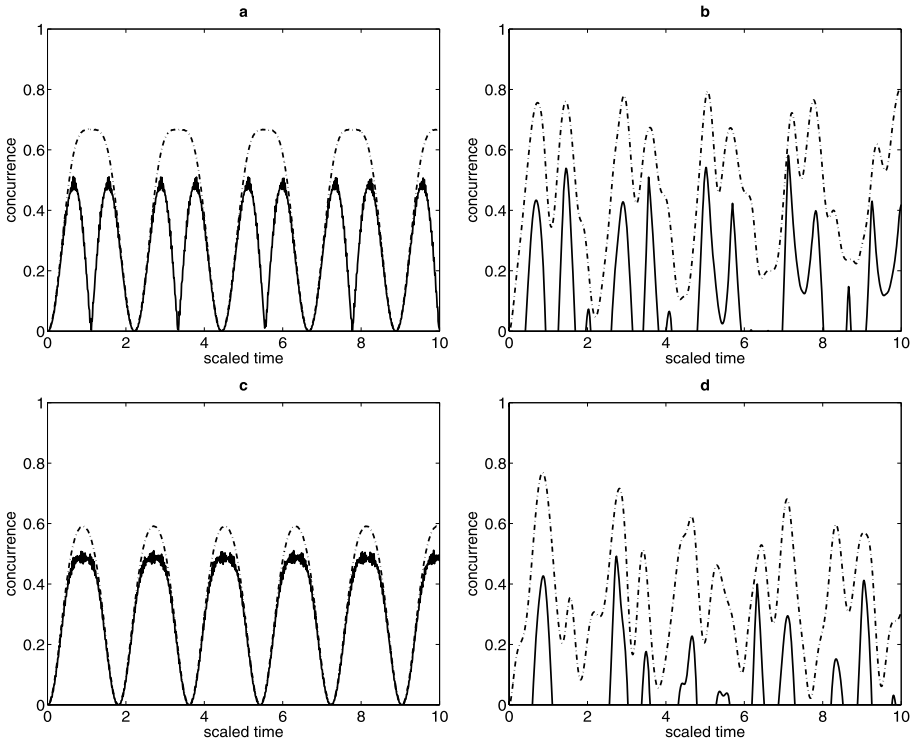


Fig. 14 The same as Fig. 13 but for $\chi/\kappa = 0.0$. (a) $r = 0.01$. (b) $r = 0.3$. (c) $\chi/\kappa = 1.0$, $r = 0.01$. (d) $\chi/\kappa = 0.5$, $r = 0.3$

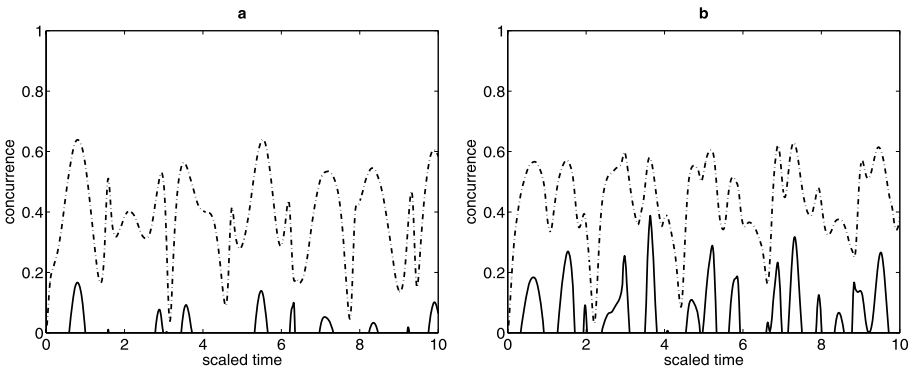


Fig. 15 The same as Fig. 13 but for $\bar{n} = 2.0$

entanglement with no decay to zero can be achieved by applying a weak Kerr medium with small level shift when the cavity is excited in the thermal state and contains only one excited atom. Furthermore, the two atoms become less entangled in excited cavity, while they become stronger entangled as well as the effects of both Kerr-like medium and Stark shift taken into consideration.

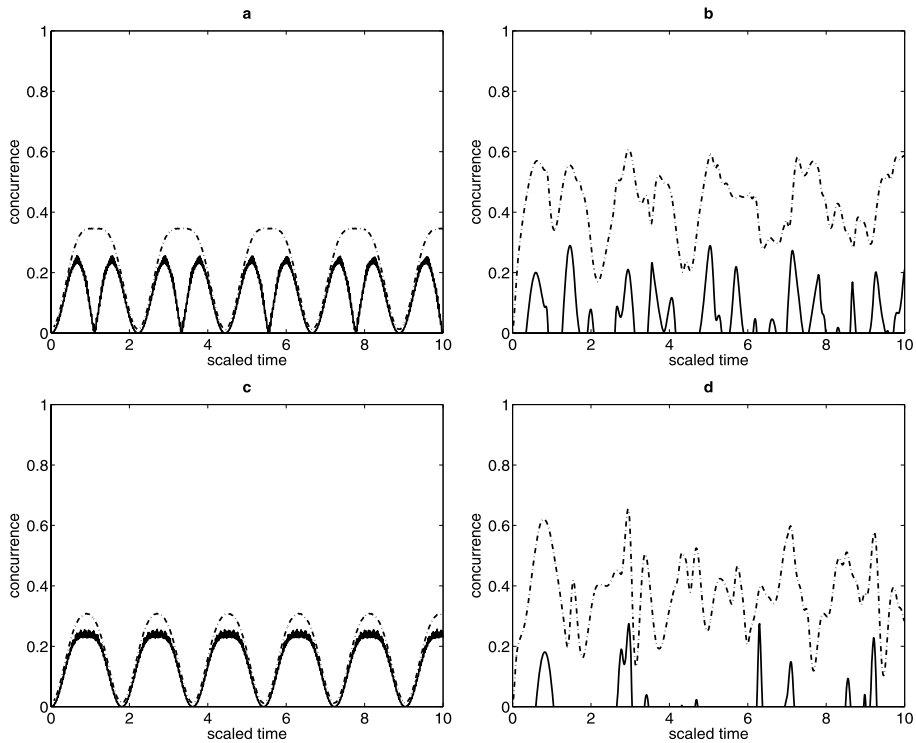


Fig. 16 The same as Fig. 14 but for $\bar{n} = 2.0$

Acknowledgements The author would like to thank the referees for their constructive comments that helped to improve the text in many ways.

References

- Nielsen, M., Chang, I.: Quantum Computation and Quantum Communication. Cambridge University Press, Cambridge (2000)
- Żukowski, M., Zeilinger, A., Horne, M.A., Ekert, A.K.: Phys. Rev. Lett. **71**, 4287 (1993)
- Bose, S., Vedral, V., Knight, P.L.: Phys. Rev. A **57**, 822 (1998)
- Bose, S., Vedral, V., Knight, P.L.: Phys. Rev. A **60**, 194 (1999)
- Shi, B.-S., Jiang, Y.-K., Guo, G.-C.: Phys. Rev. A **62**, 054301 (2000)
- Hardy, L., Song, D.D.: Phys. Rev. A **62**, 052315 (2000)
- Dür, W., Briegel, H.-J., Cirac, J.I., Zoller, P.: Phys. Rev. A **59**, 169 (1999)
- DiVincenzo, D.P., et al.: The entanglement of assistance. In: Lecture Notes in Computer Science, vol. 1509, pp. 247–257. Springer, Berlin (1999)
- Abdel-Aty, M.: J. Opt. B **6**, 201 (2004)
- Cohen, O.: Phys. Rev. Lett. **80**, 2493 (1998)
- Verstraete, F., Popp, M., Cirac, J.I.: Phys. Rev. Lett. **92**, 027901 (2004)
- Popp, M., Verstraete, F., Martin-Delgado, M.A., Cirac, J.I.: Phys. Rev. A **71**, 042306 (2005)
- Gour, G., Senders, B.C.: Phys. Rev. Lett. **93**, 260501 (2004)
- Obada, A.-S.F., Abdel-Aty, M.: Phys. Rev. B **75**, 195310 (2007)
- Gour, G.: Phys. Rev. A **71**, 012318 (2005)
- Peters, N.A., Wei, T.-C., Kwiat, P.G.: Phys. Rev. A **70**, 052309 (2004)
- Bennett, C.H., Bernstein, H.J., Popescu, S., Schumacher, B.: Phys. Rev. A **53**, 2046 (1996)
- Bennett, C.H., DiVincenzo, D.P., Smolin, J.A., Wootters, W.K.: Phys. Rev. A **54**, 3824 (1996)

19. Vedral, V., Plenio, M.B.: Phys. Rev. A **57**, 1619 (1996)
20. Vedral, V.: Rev. Mod. Phys. **74**, 197 (2002)
21. Abdel-Aty, M.: Prog. Quant. Elect. **31**, 1 (2007)
22. Vidal, G., Tarrach, R.: Phys. Rev. A **59**, 141 (1999)
23. Vedral, V., Plenio, M.B., Rippin, M.A., Knight, P.L.: Phys. Rev. Lett. **78**, 2275 (1995)
24. Wootters, W.K.: Phys. Rev. Lett. **80**, 2245 (1998)
25. Ghosh, B., Majumdar, A.S., Nayak, N.: Phys. Rev. A **74**, 052315 (2006)
26. Ghosh, B., Majumdar, A.S., Nayak, N.: Int. J. Quant. Inf. **5**, 169 (2007)
27. Cirac, J.I., Zoller, P.: Phys. Rev. A **50**, R2799 (1994)
28. Cirac, J.I., Zoller, P., Kimble, H.J., Mabuchi, H.: Phys. Rev. Lett. **78**, 3221 (1997)
29. Duan, L.-M., Lukin, M.D., Cirac, J.I., Zoller, P.: Nature Lond. **414**, 413 (2001)
30. Solano, E., Agarwal, G.S., Walther, H.: Phys. Rev. Lett. **90**, 027903 (2003)
31. Clark, S.G., Parkins, A.S.: Phys. Rev. Lett. **90**, 047905 (2003)
32. Duan, L.-M., Wang, B., Kimble, H.J.: Phys. Rev. A **72**, 032333 (2005)
33. Agarwal, G.S., Kapale, K.T.: Phys. Rev. A **73**, 022315 (2006)
34. Phoenix, S.J.D., Knight, P.L.: Phys. Rev. A **44**, 6023 (1991)
35. Phoenix, S.J.D., Knight, P.L.: Phys. Rev. Lett. **66**, 2833 (1991)
36. Kudryavtsev, I.K., Lambrecht, A., Moya-Cessa, H., Knight, P.L.: J. Mod. Opt. **40**, 1605 (1993)
37. Raimond, J.M., Brune, M., Haroche, S.: Rev. Mod. Phys. **73**, 565 (2001)
38. Matsukevich, D.N., Chaneliere, T., Jenkins, S.D., Lan, S.-Y., Kennedy, T.A.B., Kuzmich, A.: Phys. Rev. Lett. **96**, 030405 (2006)
39. Datta, A., Ghosh, B., Majumdar, A.S., Nayak, N.: Europhys. Lett. **67**, 934 (2004)
40. Tessier, T.E., Deutsch, I.H., Delgado, A.: [quant-ph/0306015](https://arxiv.org/abs/quant-ph/0306015) v4 (2003)
41. Masiak, P.: Phys. Rev. A **66**, 023804 (2002)
42. Tessier, T., Delgado, A., Fuentes-Guridi, I., Deutsch, I.H.: Phys. Rev. A **68**, 062316 (2003)
43. Hagley, E., Maitre, X., Nogues, G., Wunderlich, C., Brune, M., Raimond, J.M., Haroche, S.: Phys. Rev. Lett. **79**, 1 (1997)
44. Rauschenbeutel, A., Bertet, P., Osnaghi, S., Nogues, G., Brune, M., Raimond, J.M., Haroche, S.: Phys. Rev. A **64**, 050301 R (2001)
45. Auffeves, A., Maioli, P., Meunier, T., Gleyzes, S., Nogues, G., Brune, M., Raimond, J.M., Haroche, S.: Phys. Rev. Lett. **91**, 230405 (2003)
46. Nussmann, S., Hijlkema, M., Weber, B., Rohde, F., Rempe, G., Kuhn, A.: Phys. Rev. Lett. **95**, 173602 (2005)
47. Matsukevich, D.N., Chaneliere, T., Jenkins, S.D., Lan, S.-Y., Kennedy, T.A.B., Kuzmich, A.: Phys. Rev. Lett. **96**, 030405 (2006)
48. Kim, M.S., Lee, J., Ahn, D., Knight, P.L.: Phys. Rev. A **65**, 040101(R) (2002)
49. Zhou, L., Song, H.S., Li, C.: J. Opt. B: Quantum Semiclass. Opt. **4**, 425 (2002)
50. Braun, D.: Phys. Rev. Lett. **89**, 277901 (2002)
51. Löffler, M., Englert, B.-G., Walther, H.: Appl. Phys. B **63**, 511 (1996)
52. Majumdar, A.S., Nayak, N.: Phys. Rev. A **64**, 013821 (2001)
53. Rempe, G., Schmidt-Kaler, F., Walther, H.: Phys. Rev. Lett. **64**, 2783 (1990)
54. Rempe, G., Walther, H.: Phys. Rev. A **42**, 1650 (1990)
55. Paul, H., Richter, Th.: Opt. Commun. **85**, 508 (1991)
56. Cresser, J.D.: Phys. Rev. A **46**, 5913 (1992)
57. Phoenix, S.J.D., Barentt, S.M.: J. Mod. Opt. **40**(6), 979 (1993)
58. Filipowicz, P., Javanainen, J., Meystre, P.: Phys. Rev. A **34**, 3077 (1986)
59. Phoenix, S.J.D., Knight, P.L.: Ann. Phys. **186**, 381–407 (1988)
60. Meschede, D., Walther, H., Muller, G.: Phys. Rev. Lett. **54**, 551 (1985)
61. Filipowicz, P., Javanainen, J., Meystre, P.: J. Opt. Soc. Am. B **3**, 906 (1986)
62. Lipeles, M., Novick, R., Tolk, N.: Phys. Rev. Lett. **15**, 690 (1965)
63. Mcneil, K.J., Walls, D.F.: J. Phys. A **7**, 617 (1974)
64. Nayak, N., Mohanty, B.K.: Phys. Rev. A **19**, 1204 (1979)
65. Moya-Cessa, H., Knight, P.L., Rosenhouse-Dantsker, A.: Phys. Rev. A **50**, 1814 (1994)
66. Yuen, H.P.: Phys. Rev. A **13**, 2226 (1976)
67. Caves, C.M.: Phys. Rev. D **23**, 1693 (1981)
68. Fang, M.-F., Liu, H.-E.: Phys. Lett. A **200**, 250 (1995)
69. Abdel-Aty, M., Furuichi, S., Ateto, M.: Jpn. J. Appl. Phys. **41**, 111 (2002)
70. Wang, C.-Z., Li, C.-X., Guo, G.-C.: Eur. Phys. J. **37**, 267 (2006)
71. Abdel-Aty, M., Abdel-Khalek, S., Obada, A.-S.F.: Chaos, Solit. Fract. **12**, 2015 (2001) (and papers therein)
72. Joshi, A., Puri, R.R.: Phys. Rev. A **45**, 5056 (1992)

73. Hillery, M.: Phys. Rev. A **44**, 4578 (1991)
74. Chaba, A.N., Collett, M.J., Walls, D.F.: Phys. Rev. A **46**, 1499 (1992)
75. Zambrini, R., Hoyuelos, M., Gatti, A., Colet, P., Lugiato, L., Miguel, M.S.: Phys. Rev. A **62**, 063801 (2000)
76. Gerry, C.C.: Phys. Rev. A **59**, 4095 (1999)
77. Paternostro, M., Kim, M.S., Ham, B.S.: Phys. Rev. A **67**, 023811 (2003)
78. Pachos, J., Chountasis, M.: Phys. Rev. A **62**, 052318 (2000)
79. Vitali, D., Fortunato, M., Tombesi, P.: Phys. Rev. Lett. **85**, 445 (2000)
80. Ateto, M.S.: Int. J. Quant. Inf. **5**(4), 535 (2007)
81. Englert, T., Gantsog, B.-G., Schenzle, A., Wagner, C., Walther, H.: Phys. Rev. A **53**, 4386 (1996)
82. Maitre, X., Hagley, E., Nogues, G., Wunderlich, C., Goy, P., Brune, M., Raimond, J.M., Haroche, S.: Phys. Rev. Lett. **79**, 769 (1997)
83. Englert, B.-G., Lougovski, P., Solano, E., Walther, H.: e-print: [quant-ph/0209128v1](https://arxiv.org/abs/quant-ph/0209128v1) 24Sep (2002)
84. Horodecki, R., Horodecki, P., Horodecki, M.: Phys. Lett. A **200**, 340 (1995)
85. Fang, M.-F., Liu, H.-E.: Phys. Lett. A **210**, 11 (1996)